

SOS model of overlayer induced faceting

Czesław Oleksy*

*Institute of Theoretical Physics, University of Wrocław,
Plac Maksa Borna 9, 50-204 Wrocław, Poland*

(Dated: March 4, 2003)

A solid-on-solid model is proposed to describe faceting of bcc(111) metal surface induced by a metal overlayer. It is shown that the first order phase transition occurs between faceted {211} or {110} and disordered phases. The ordered phases consist of large 3-sided pyramids with {211} facets or {110} facets. It is shown that the high-temperature disordered phase has not planar bcc(111) structure but faceted disordered structure. Hysteresis effects were observed when the system was warmed above the transition temperature and then cooled down. Temperature dependence of LEED patterns for faceted and disordered phase are calculated in kinematic approximation.

PACS numbers: 68.35.Rh, 68.43.De, 64.60.Cn

I. INTRODUCTION

Recent experiments^{1,2,3,4,5,6,7} have demonstrated that surfaces such as W(111) and Mo(111) covered by a single physical monolayer of certain metal, e.g., Pd, Pt, undergo massive reconstruction from planar morphology to microscopically faceted surface after annealing to $T > 700K$. The reconstructed surface consists of 3-sided pyramids with mainly {211} facets, and pyramid dimensions range from ~ 1 to 100 nm. It has been shown that facets are composed of substrate atoms, and the monolayer of adsorbate remains on the outermost surface layer during the faceting transformation. Another type of massive reconstruction has been very recently found in STM and LEED experiment for Pd on Ta(111) system⁸. The reconstructed surface consists of {011} facets which form large triangular pyramids. The third type of reconstructed structure, coexistence of small {011} facets with large {211} facets, has been observed² in Pd on W(111) for prolonged annealing time (for short annealing time only {211} pyramids occurred). An important step in understanding the thermal stability of reconstructed surfaces was LEED experiment performed in high temperatures for Pd on Mo(111) by Song et al.⁷. They demonstrated existence of reversible phase transition between faceted {211} and planar phases and they found that this transition has a large hysteresis, i.e., the transition temperature in cooling cycle ($T \approx 830$) is lower than that in the heating cycle ($T \approx 870$).

In theoretical studies of overlayer-induced faceting^{2,9,10} the first principle method have been used to calculate the surface formation energy of fcc metals (Pd, Pt, Au, Ag, Cu) adsorbed on Mo and W. Results of these calculation performed for pseudomorphic adsorbate overlayer on (111), (211), and (011) flat surfaces show that (111) surface becomes unstable at the coverage of one physical monolayer, where the energy of (211) orientation has the lowest value. However, such energy calculation (at $T=0$) are not sufficient to explain why some of these metals do not induce faceting, e.g., Ag/Mo(111). On the other hand, the first principle calculation confirmed that critical coverage to induce faceting is approximately equal to

one physical monolayer (PML) and that the growth mode is Stransky-Krastanov as the surface energy increases at coverage higher than 1 PML.

Theoretical studies of surface reconstruction and surface phase transitions in bimetallic system are complicated problems mainly due to occurrence of long range many-body interactions. One of approaches to such problems is application of simple solid-on-solid models^{11,12,13,14}, in which the crystal is represented by two-dimensional array of columns. They were employed to study roughening transition^{11,12}, missing-row reconstruction¹⁵, growth of the surface¹², surface diffusion^{12,16}, adsorption¹⁴, phase transitions in two component crystal¹³, etc.

In this paper we introduce a simple SOS model for bcc(111) surface covered by one physical monolayer of adsorbed atoms to describe surface reconstruction and phase transitions. Using Monte Carlo simulation we study change of the surface structure during the heating and cooling processes, phase transitions to a faceted phases, phase diagram, LEED patterns and temperature dependence of diffracted intensity calculated in kinematic approximation.

II. THE SOS MODEL

To study faceting in bimetallic system one needs to know interaction potentials. There are many-body potential for Mo-Mo and W-W interactions derived by Finnis and Sinclair¹⁷ but to our knowledge there is only Ni-Mo many-body potential¹⁸ for interaction between (Mo, W) and fcc metals. However in Ni/Mo(111) system the faceting does not occur³. Therefore we are going to study overlayer induced faceting using a simple solid-on-solid (SOS) model which describe a surface formation energy in agreement with result of the first principle calculation.

In order to construct a model of overlayer-induced faceting on bcc(111) surface (BCCSOS) we are taking into account some experimental evidences. There is a critical coverage, approximately equal to 1PML, to induce faceting on W(111) and Mo(111)⁴. When the cover-

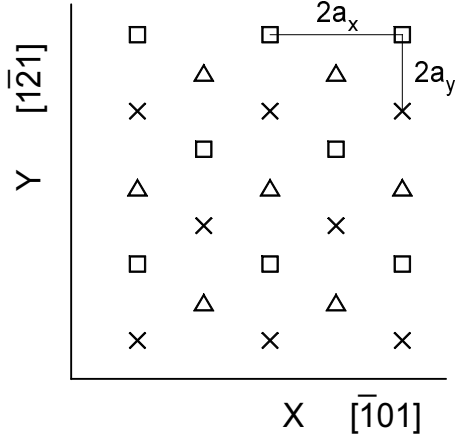


FIG. 1: Schematic view of the bcc(111) surface. Sites of the sublattices $l = 0, 1, 2$ are denoted by squares, triangles, crosses, respectively. The Z axis is normal to the plane and $a_x = a\sqrt{2}/2$, $a_y = a\sqrt{6}/6$.

age exceeds 1PML, extra adsorbate atoms form 3D clusters on the top of faceted surfaces. Hence to simplify problem it will be assumed that coverage is constant and equal to 1PML. Such coverage is equivalent to 3, 2, and 1 geometric monolayers of adsorbate on bcc (111), (211), and (011) surfaces, respectively. A second assumption is that substrate atoms (B) can take position in discrete bcc lattice. It has been shown², in the case of Pd/W(111), that both $\{011\}$ facets and $\{112\}$ facets of W are covered by pseudomorphic monolayer of Pd. Therefore we assume that adsorbate atoms (A) are also located in positions of the bcc structure. There are three types of interaction energies in this SOS model: adsorbate-adsorbate interaction ϵ_i^{AA} , adsorbate-substrate interaction ϵ_i^{AB} , and substrate-substrate interaction ϵ_i^{BB} , with the range of interaction up to forth neighbors ($i = 1, 2, 3, 4$).

It is convenient to chose the coordinate system with the Z axis parallel to $[111]$ direction and X, Y axes along $[\bar{1}01]$, $[121]$ directions in the (111) plane. Atoms along the closed packed direction (parallel to the z axis) form columns which positions in the (x, y) plane are described by three triangular sublattices $l = 0, 1, 2$ shown in Fig. 1. Column height z_i at site i in the l th sublattice is defined as $z_i = h_i a \sqrt{3}/6$ where a is bcc lattice constant, $h_i = 3n_i + l$ and n_i is the number of atoms in i th column. The assumption on constant coverage equal to 1PML means that there is exactly one A atom in each column placed on its top. As we are going to study reconstruction only, not desorption or crystal melting, the typical restriction of SOS models on columns heights will be assumed. The h_i difference between nearest neighbor sites are forced to be $\pm 1, \pm 2$.

Let us define the Hamiltonian as surface formation energy of A material on B (111) surface

$$H = E_{A/B}(N_A, N_B) - E_A^{bulk}(N_A) - E_B^{bulk}(N_B), \quad (1)$$

where $E_{A/B}(N_A, N_B)$ denotes energy of N_A atoms A on bcc(111) surface consisting of N_B atoms B, $E_A^{bulk}(N_A)$, $E_B^{bulk}(N_B)$ are energies of A, B atoms in their bulk environments. Now taking into account above assumptions we can express Hamiltonian Eq. (1) in terms of column heights h_i in the following form

$$H = \frac{1}{2} \sum_i \left\{ \sum_{j_1} [J_1 \delta(|h_i - h_{j_1}| - 1) + K_1 \delta(|h_i - h_{j_1}| - 2)] \right. \\ + \sum_{j_2} [2J_2 \delta(|h_i - h_{j_2}|) + (2J_2 + K_2) \delta(|h_i - h_{j_2}| - 3)] \\ \left. + J_2 \sum_{j_3} [\delta(|h_i - h_{j_3}| - 2) + \delta(|h_i - h_{j_3}| - 4)] \right\} + N J_0, \quad (2)$$

where

$$J_0 = -\frac{1}{2} \epsilon_1^{BB} + \epsilon_1, \\ J_1 = -\frac{1}{2} (\epsilon_2^{BB} + \epsilon_3^{BB} + 2\epsilon_4^{BB}) + \epsilon_2 + \epsilon_3 + \epsilon_4, \\ K_1 = -\frac{1}{2} (\epsilon_1^{BB} + 2\epsilon_3^{BB} + \epsilon_4^{BB}) + \epsilon_1 + \epsilon_3 + \epsilon_4, \\ J_2 = -\frac{1}{2} \epsilon_4^{BB} + \epsilon_4, \\ K_2 = -\frac{1}{2} \epsilon_3^{BB} + \epsilon_3 - \epsilon_4, \\ \epsilon_i = \epsilon_i^{AB} - \epsilon_i^{AA},$$

and sums over j_1, j_2 , and j_3 denotes summing over first, second, and third neighbors of a column at site i . In what follows, we will treat J_1, J_2, K_1 , and K_2 as model parameters. It is worth noting that this BCCSOS Hamiltonian of overlayer-induced faceting at constant coverage can also be used to study a clean bcc(111) surface by setting $\epsilon_i^{AB} = \epsilon_i^{AA} = \epsilon_i^{BB}$.

A. Energies of (111), (211), and (110) faces at $T=0$

First, we will check the stability of ideal surfaces (111), (211), and (110) covered with 3, 2, 1 geometric monolayers of A, similarly as it was performed in first principles calculations⁹. This allows us to estimate values of model parameters for reconstruction, from (111) surface to $\{112\}$ or to $\{011\}$ faceted surface, under assumption that edge energies are neglected.

Using the Hamiltonian Eq. (2) we get the following expressions for surface energy per site for ideal face of orientation (hkl)

$$E_{111} = E_r + 7J_2, \\ E_{110} = E_{111} + 2J_2 + 2K_2, \\ E_{211} = E_{111} + K_2, \\ \text{where} \\ E_r = J_0 + K_1 + 2J_1.$$

Thus, the stability conditions are:

$$\begin{aligned} K_2 &\geq 0, J_2 + K_2 \geq 0 && \text{for (111) surface,} \\ J_2 + K_2 &\leq 0, 2J_2 + K_2 \leq 0 && \text{for (110) surface,} \\ K_2 &\leq 0, 2J_2 + K_2 \geq 0 && \text{for (211) surface.} \end{aligned}$$

It is easy to see that transformation from (111) surface to {211} facets will be possible for negative values of K_2 and appropriate positive J_2 . To satisfy these conditions, the range of interactions $\epsilon_i^{\alpha\beta}$ should be not smaller than $r_4 = a\sqrt{11}/2$. On the other hand, it is easy to ensure stability of bcc(111) surface at zero coverage ($\epsilon_i = 0$) by choosing $\epsilon_3^{BB} < 0$ and $\epsilon_4^{BB} < 0$. Thus, there is general possibility to choose a set of interactions $\{\epsilon_3^{BB}, \epsilon_4^{BB}, \epsilon_3, \epsilon_4\}$ in such a way that at zero coverage the bcc(111) surface is stable whereas for coverage equal to one physical monolayer the bcc(211) surface becomes stable.

It is worth noting that surface energies per site E_{hkl} are related to surface energies per surface atom σ_{hkl} (used in first principles calculation^{2,9}) in the following way $\sigma_{111} = 3E_{111}$, $\sigma_{211} = 2E_{211}$, $\sigma_{110} = E_{110}$, as the number of surface atoms is $N/3$, $N/2$, and N , respectively. Moreover, above stability conditions correspond to faceting conditions^{2,9} expressed in terms of scaled σ_{hkl} , e.g., the conditions $E_{211} \leq E_{111}$, $E_{211} \leq E_{110}$ are equivalent to $3\sigma_{211}/2 \leq \sigma_{111}$, $3\sigma_{211}/2 \leq 3\sigma_{110}$ for transformation $\{111\} \rightarrow \{112\}$.

Independence of stability condition on parameters J_0 , J_1 , and K_1 comes from assumptions on constant number of adsorbate atoms A and the restriction on column heights. Therefore we neglect these parameters in further analysis what corresponds to shifting of the surface energy by $-E_r$. Moreover, by choosing J_2 as the unit of energy we will work with dimensionless quantities: energy $\tilde{H} = H/J_2$, temperature $\tilde{T} = k_B T/J_2$, and parameter $\tilde{K} = K_2/J_2$ (in what follows, the tilde will be omitted).

III. SIMULATION OF FACETING

We will discuss here results of the annealing process investigated by Monte Carlo (MC) simulation in canonical ensemble. Let us start with some details concerning the simulation method. Configurations of BCCSOS model are generated via the classic Metropolis algorithm. A new configuration in Markov chain is generated from the previous configuration by moving one B atom from a site i to a site j , what is equivalent to the following change of heights: $(h_i, h_j) \rightarrow (h_i - 3, h_j + 3)$. It is important to note that such change of heights is possible only if h_i is the local maximum (with respect to the nearest neighbors) and h_j is the local minimum because of the restriction on column heights. Let us remember one of the model assumptions that adsorbate atoms always stay on the column tops as we study reconstruction of B surface covered by the physical monolayer of A material. MC simulation was carried out on rectangular lattice of linear size L_x, L_y along x, y direction, respectively with periodic boundary conditions (PBC). To check the role of PBC additional simulations were performed with bound-

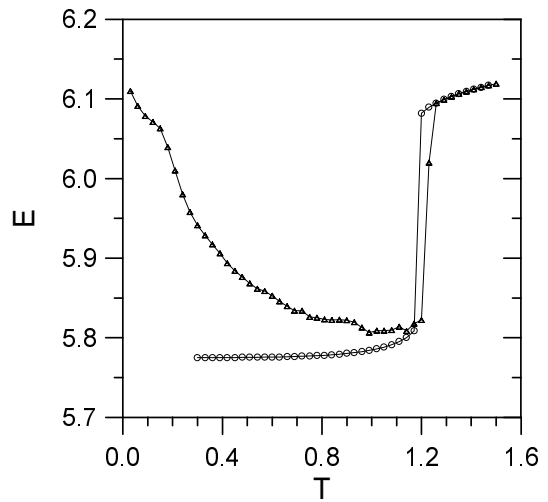


FIG. 2: Temperature dependence of the surface energy during the warming up cycles (triangles) and the cooling cycles (circles).

ary atoms fixed at positions of the flat bcc(111) surface. The results are consistent with those obtained for calculation with PBC.

First, we investigate properties of the system with coupling constant $K = -1.25$ during warming up process. At each temperature $T_i = T_{i-1} + \Delta T$ system spends the same annealing time τ measured in Monte Carlo steps per site. The ideal bcc(111) surface is used as a starting configuration at T_0 . We also investigate properties of the system during cooling down the sample. Results of simulations for the following parameters: $L_x = 192$, $L_y = 336$, $\Delta T = 0.03$ and $\tau = 3 \times 10^5$ are presented in Fig. 2-Fig. 5. Let us notice that these sizes of the lattice correspond to the area of $426\text{\AA} \times 431\text{\AA}$ on the bcc(111) surface with the lattice constant $a = 3.14\text{\AA}$.

The surface formation energy decreases as temperature is elevated (see Fig. 2) what indicates reconstruction of the surface. At $T \approx 0.4$ very small 3-sided {211} pyramids are formed on the surface and further warming up causes growth of pyramids sizes (see Fig. 3). By the {211} pyramid we mean the pyramid built of (211), (121), and (112) facets. A big jump of the surface energy is observed at $T = 1.26$ where the phase transition to disordered phase occurs. On the other hand, discontinuous change of the surface energy is observed at $T = 1.20$ when the system is cooling down. The hysteresis loop seen in Fig. 2 indicates that the phase transition is of first order. The surface is undercooled or overheated because system rests in metastable state separated from the stable state by the free energy barrier. The hysteresis effects, dependence of temperature of the phase transition on cooling and warming, has been observed in LEED experiment⁷ for Pd/Mo(111). When system is cooling down we observe formation of large pyramids with defected faces and edges just below the temperature of the phase transition (see Fig. 4). Facets of similar shapes and sizes were ob-

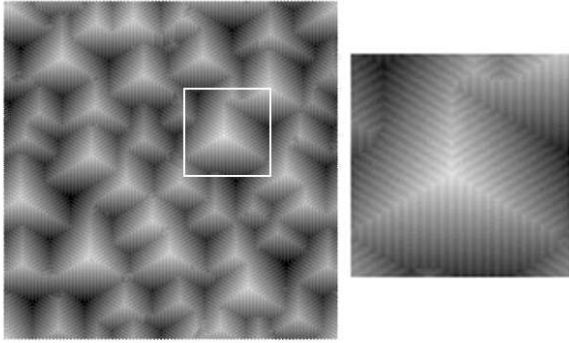


FIG. 3: Snapshot of the surface at $T=0.72$ on warming.

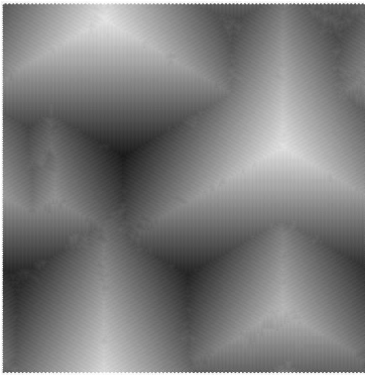


FIG. 4: Snapshot of the surface at $T=1.17$ on cooling.

served at this temperature on warming. During further cooling defects disappear and pyramids take nearly ideal shapes at $T \approx 1$. Therefore the dependence of surface energy on cooling is very weak in the ordered faceted phase.

It is very interesting that in the disordered phase the surface is not planar as suggested in experimental works⁷. The structure of disordered phase contains randomly distributed small facets mainly of $\{112\}$ orientations what is shown in Fig. 5 where the cross section of the disordered phase is compared to cross sections of faceted $\{211\}$ and ideal bcc(111) surfaces. Moreover, we calculated the average number of atoms on a facet of orientation (211) which in the disordered phase is nearly 10. So we will call this phase as disordered faceted phase (DFP). In very narrow temperature range, we observed a coexistence of a faceted $\{112\}$ and DFP, e.g., in simulation at $T = 1.23$ denoted by the triangle in Fig. 2. A surface structure in this case looks like surface of ordered phase where large pyramids are removed and on their place DFP is present. On the other hand, there are 3-sided pyramidal holes built of large facets of $\{112\}$ orientation. Sometimes, DFP is located also at the bottom of these holes. It is worth noting that coexistence of both faceted and

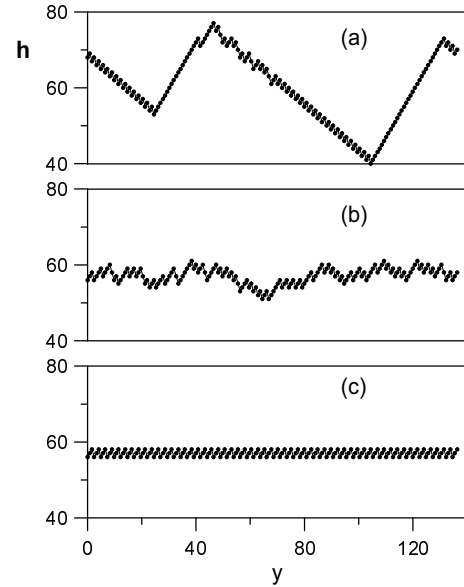


FIG. 5: Plot of column height along the y direction for the surface: (a) below the phase transition, $T=1.17$, (b) above the phase transition, $T=1.50$, (c) ideal bcc(111) - initial configuration.

disordered phases has been observed⁷ in LEED experiment in Pd/Mo(111) system. However, it was suggested that coexistence is due to the inhomogeneity of the surface.

One of quantities measured in MC simulation is the square mean width of the surface,

$$\delta h^2 = \left\langle \frac{1}{N} \sum_j (h_j - \langle h \rangle)^2 \right\rangle. \quad (3)$$

Behaviour of the δh^2 during warming up and cooling down processes allows us to study dependence of mean vertical sizes of pyramids on temperature. In Fig. 6 we present results of simulation for 3 different annealing times $\tau = 2 \times 10^3$, 2×10^4 , 3×10^5 . In all cases the hysteresis loop is present near the phase transition and for shorter time a larger hysteresis is observed. It is easy to explain because it is more probable to overcome the free energy barrier in longer time. In the warming up process the size of pyramids does not depend on the annealing time τ up to $T \approx 0.5$. When temperature approaches $T \approx 1$ then a rapid growth is observed and for longer annealing time τ greater pyramids are formed on the surface. Pyramids reach maximal sizes just below the temperature of the phase transition where dependence of sizes on annealing time is the strongest. It is worth noting that dependence of facets size on temperature qualitatively agrees with the experimental results⁴. The value of δh^2 rapidly decreases above the phase transition where very weak dependence on temperature is observed. In the cooling down process large pyramids are formed just below the phase transition temperature, and further de-

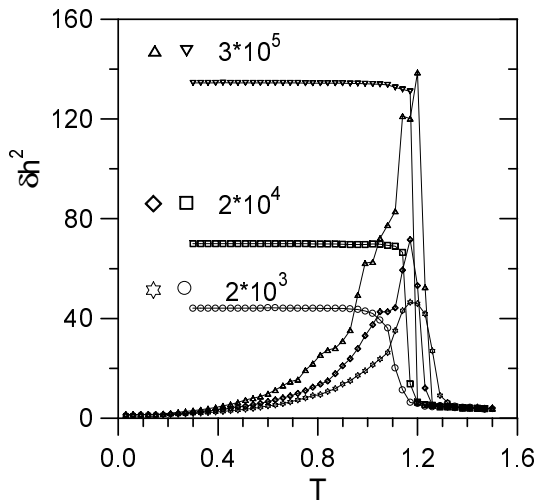


FIG. 6: Temperature dependence of the δh^2 during the heating and the cooling cycles for 3 different annealing times. Each label contains symbols for heating, cooling and the number of MC steps

creasing of temperature practically does not change the size of pyramids.

We check dependence of surface growth on the initial temperature T_0 and we find that the behaviour of δh^2 near the transition point is very similar to that in Fig. 6 for process which starts at $T_0 = 0.3$ or $T_0 = 1.0$. Finally we analyze the influence of the temperature increment, ΔT , on the surface energy and the δh^2 near the phase transition for $\tau = 3 \times 10^5$. We found that for $\Delta T = 0.01$ the hysteresis loop slightly increases, there are more points where the faceted and disordered phases coexist but it seems that sizes of pyramids do not depend on the temperature increment.

We observe that the growth of the facets on warming base on formation of a larger pyramid from several smaller pyramids. Probability of such rebuilding of the surface is very small at low temperature. This is reflected in the acceptance ratio f , a fraction of accepted configurations in the Markov chain, which is very low at low temperatures, $f \approx 0.002$ below $T = 0.3$ and $f = 0.01$ at $T = 0.7$. On the other hand, the acceptance ratio is of the same order for $T = 1.0$, $f = 0.1$, and close to the phase transition, $f = 0.2$, but we observe difference in facets sizes at these temperatures. Looking at snapshots of the surface after annealing at temperature up to $T \approx 1.1$ on warming, we found that pyramids have nearly ideal shapes (see for example Fig. 3). We think that all above observation can be explained in the following way. The system is passing through metastable states - local minima of the free energy - as temperature is increased. There are barriers between local minima hence the growth of facets depends on the annealing time.

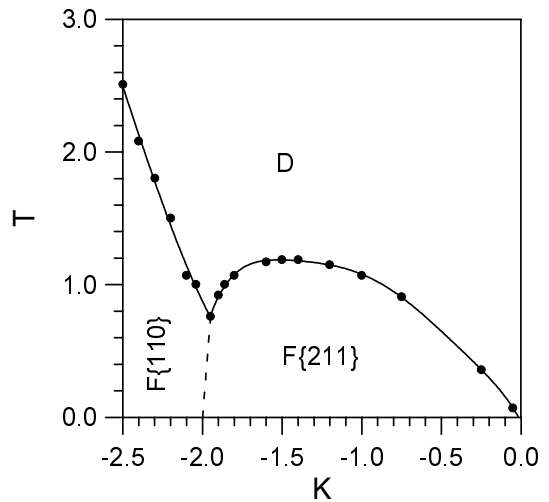


FIG. 7: Phase diagram: T versus K .

IV. PHASE DIAGRAM

The stability analysis of flat (111), (211), and (110) surfaces in Sec. II A shows that at $T = 0$ the (211) surface is stable for $-2 \leq K < 0$ whereas for $K < -2$ the (110) surface is stable. Whether these findings are generally correct we can check constructing phase diagram in the (T, K) plane by using MC simulations. Most of simulations were performed at constant K varying temperature. To check the results some simulations were performed at constant temperature. To identify different phases we calculated masses of clusters of different facet orientations (111), {110}, and {112}. A cluster of orientation (hkl) is defined in similar way as percolation cluster on the (hkl) plane. We also recorded equilibrium configurations at each investigated point of the (T, K) plane. We found that for $K < 0$ the phase diagram (see Fig. 7) contains three phases

1. Faceted {112} phase consisting of 3-sided {112} pyramids.
2. Faceted {110} phase consisting of 3-sided {110} pyramids.
3. Disordered faceted phase.

The surface of the faceted {110} phase is built of (110), (101), and (011) facets which form 3-sided pyramids on the bcc(111) surface. Such surface has been observed experimentally in Pd on Ta(111) system⁸. The phase transition between the disordered phase and one of ordered is of first order as surface energy, the square mean width of the surface δh^2 , and the structure factor (see Sec. V) change discontinuously at the transition point. The transition temperature between F{211} and disordered phase is bounded from above by maximum $T_c = 1.20$ at $K = -1.50$. If we chose this point to estimate model parameters for Pd/Mo(111) with $T_c = 850$ K we get

$J_2 = 0.06$ eV, and $K_2 = -0.09$ eV. On the other hand the transition temperature from $F\{110\}$ to the disordered phases is increasing function of $|K|$ and it might reach large value. The present model does not include the desorption, thus we can expect that transition temperature might be above the desorption temperature in some systems especially where the faceted $F\{110\}$ phase occurs. In such cases the phase transition to the disordered faceted phase could not be observed but rather deconstruction induced by desorption would be expected.

There is difficult to study phase transition between ordered phases using MC simulation because for $K \approx -2$ we observed coexistence of two types of facets $\{011\}$ and $\{112\}$. The mixed phase does not contain separated pyramids of two types but mixture of facets, e.g., on the (211) facet a smaller (011) facet can occur.

V. SIMULATION OF LEED PATTERNS

Low energy electron diffraction (LEED) experiments play an important role in investigation of structures and phase transitions of faceted surfaces^{4,7}. Very recently, Song et al.⁷ were able to study LEED patterns of Pd/Mo(111) system in high temperatures up to 1200K. They demonstrated the existence of reversible planar/faceted phase transition with transition temperature different for heating cycles ($T \approx 870K$) and for cooling cycles ($T \approx 830K$).

In this section we employ the BCCSOS model to analyze the temperature dependence of LEED patterns. The diffracted intensity is proportional, in the kinematic approximation, to the structure factor

$$S(\mathbf{k}) = \left\langle \left| \sum_j \exp(i\mathbf{k}\mathbf{R}_j) \right|^2 \right\rangle, \quad (4)$$

where summing is over surface atoms, $\mathbf{k} = \mathbf{k}_f - \mathbf{k}_i$, and \mathbf{k}_i , \mathbf{k}_f is the wave vector of incident electron, scattered electron, respectively. Position of surface atoms \mathbf{R}_j is expressed by column height h_{r_j} in site $r_j = (x_j, y_j)$ in the following way $\mathbf{R}_j = a(3\sqrt{2}x_j, \sqrt{6}y_j, \sqrt{3}h_{r_j})/6$. In a SOS model not all atoms from column tops are surface atoms. Therefore in calculation of diffracted intensity sometimes the shadowing factor is used¹⁵. In this paper we consider the contribution to S only from surface atoms. As a surface atom in any configuration we choose the atom from the top of column which has at least four lower nearest neighbors. In the case when number of higher columns is equal to 3 then atom is regarded as surface atom if is not surrounded by the higher neighbors. Such case occurs for atoms on $\{110\}$ facets. We will calculate structure factor only for a set of \mathbf{k}_f , chosen in such a way to describe diffraction on faces $\{111\}$ and $\{211\}$. For each of these faces we construct a pair of inverse lattice vectors $\mathbf{g}_1, \mathbf{g}_2$ parallel to the face, e.g., for (121) $\mathbf{g}_1 = 2\pi/a(\sqrt{2}/2, 0, 0)$

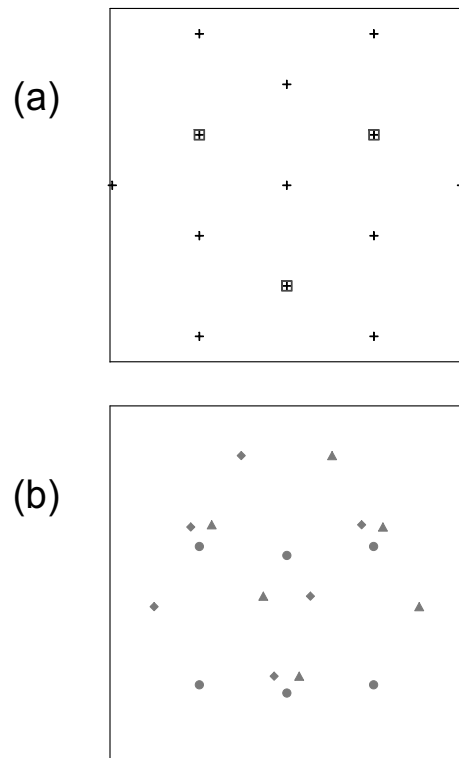


FIG. 8: LEED patterns of (a) disordered phase where spots are represented by squares and also spots of ideal bcc(111) surface (crosses) are shown, (b) faceted $\{211\}$ phase where circles, diamonds, and triangles denote spots coming from diffraction on facets (121), (211), and (112), respectively.

and $\mathbf{g}_2 = 2\pi/a(0, 4\sqrt{6}/9, 2\sqrt{3}/9)$. Then, the wave vectors of scattered electrons, \mathbf{k}_f , for given face are chosen to satisfy condition of constructive interference $(\mathbf{k}_f - \mathbf{k}_i)_{\parallel} = l\mathbf{g}_1 + m\mathbf{g}_2$, where $l, m = 0, \pm 1, \dots$ and the symbol \parallel denotes vector component parallel to the face.

We calculated structure factors for the wave vector of the incident electron, $k_i = 2\pi/a(0, 0, 1.43)$, normal to the bcc(111) surface. Thus energy of incident electrons is equal to 31 eV for $a = 3.14\text{\AA}$, similarly as in LEED experiment for Pd/Mo(111)⁷. Figure 8 shows LEED patterns obtained in computer simulation for the model parameter $K = -1.25$. In the ordered phase $\{211\}$ we see besides 3 clovers (groups of 3 spots) observed experimentally, the fourth clover in the center of the image, and six single spots more distant from the center. The pattern of disordered phase consists of three spots which positions correspond to the centers of external clovers in the diffracted pattern of the faceted phase. Apparent lack of spots from bcc(111) surface confirms that disordered phase has not the planar structure.

Temperature dependence of the structure factors were calculated using MC simulation and changing temperature in the way described in Sec. III. Most of simulations were performed on the lattice with $Lx = 90$, $Ly = 132$. The spots of disordered phase have the same diffracted intensities. Their temperature dependence (see Fig. 9) on

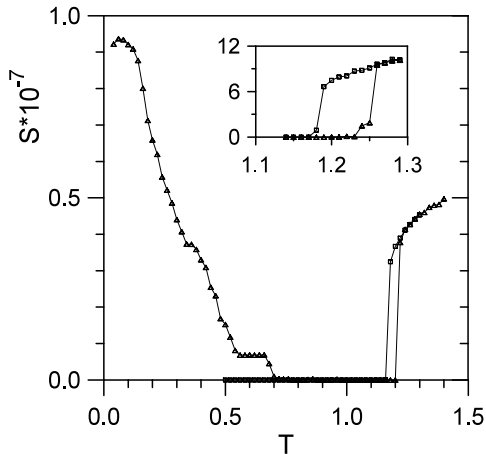


FIG. 9: Temperature dependence of the structure factor for the wave vector corresponding to a spot of the disordered phase on warming (triangles) and on cooling (squares). The hysteresis loop for large lattice $Lx = 192, Ly = 336$, is shown in the inset.

warming and on cooling shows the presence of hysteresis loop in behaviour of $S(T)$ close to the phase transition what is in agreement with experimental results⁷. The hysteresis loop calculated for large lattice with $Lx = 192, Ly = 336$ is shown in the inset in Fig. 9. There are several points where the structure factor takes intermediate values because at these temperatures coexistence of faceted and disordered phases has been observed. More coexistence points were found on warming than on cooling. We observe also discontinuity of the structure factor at the transition temperature. Thus hysteresis and discontinuity of the structure factors are another argument for the first-order phase transition between faceted and disordered phases. During the process of warming up the system the S decreases with temperature and becomes very small when on the surface large enough $\{211\}$ facets are formed.

The diffracted intensities of a spot in the ordered phase was calculated for \mathbf{k}_f fulfilling the condition of constructive interference and also for vectors from a very small surroundings of \mathbf{k}_f . Then maximal value of S were chosen to represent the intensity of spot at this \mathbf{k}_f . We use such procedure because the surface does not consist of ideal flat $\{211\}$ facets during warming up and cooling processes, therefore spots can change shapes, intensities, and positions. The diffracted intensities of spots of faceted phase are different because areas of facets of different orientation are not equal. Moreover, their dependence on temperature during warming the system shows irregular behaviour (see Fig. 10) because of facets grow i.e., from several small facets a bigger one arises. We observe rapid growth of S at temperature $T \approx 0.9$ when large pyramids are formed on the surface. During the cooling cycles, the S reaches nearly maximal value just

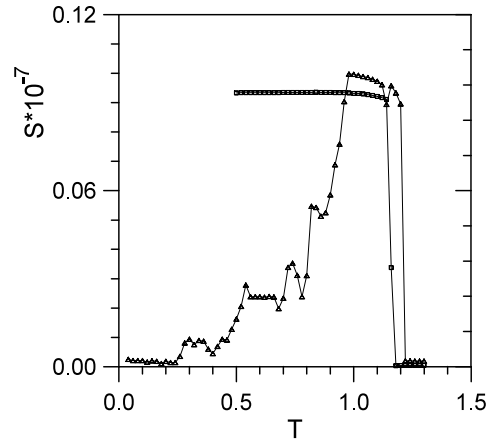


FIG. 10: Temperature dependence of the structure factor for the wave vector corresponding to a leaf of the right clover on warming (triangles) and on cooling (squares).

below transition temperature what confirms formation of large $\{211\}$ facets. The maximal values of S in the faceted phase are nearly ten times smaller than in the disordered phase because in former case only $\sim 1/3$ surface atoms contribute to S , i.e., surface atoms placed on facets of the same orientation.

VI. DISCUSSION

We have presented here the BCCSOS model to study overlay induced faceting. Although it might seem that model is very simple it gives many results in agreement with experiments. It has been shown that bcc(111) surface covered by a physical monolayer undergoes reconstruction upon annealing. We obtained two types of reconstructed surfaces: faceted $\{211\}$ covered by 3-sided pyramids as observed in Pd/Mo(111)³ and faceted $\{011\}$ surface found in Pd/Ta(111)⁸. The sizes of facets depend on annealing temperature and annealing time. At high temperature the phase transition to disordered phase occurs. We have shown that LEED diffraction patterns can be calculated, in kinematic approximation, in warming up and cooling down processes for different electron energies. In dependence of diffracted intensities on temperatures the hysteresis effect was observed close to temperature of the phase transition.

On the other hand, we can investigate some properties not reported in experimental papers. First of all the phase transition can be studied in details using this model. It is shown that the phase transition is of first order because quantities such as surface energy, the structure factor change discontinuously as temperature reaches the transition point. Moreover the hysteresis effects are observed when system is warming up and then cooling down. We can analyze the structure of the surface

in disordered phase as well as in the coexistence of the faceted and disorder phase close to the transition temperature. We found that the disordered phase consists of many small $\{211\}$ facets randomly distributed. Hence it is not planar bcc(111) surface. It would be interesting to check experimentally this prediction. It was suggested⁷ that coexistence of faceted and disordered phases is due to the inhomogeneity of the adsorbate coverage but we have demonstrated that the coexistence could also exist for homogeneous coverage.

It seems that this model can be applied to study reconstruction of curved bcc surfaces where reconstructed surface has different structure than faceted bcc(111) surface. In case of Pd deposited on a needle-shaped tungsten¹⁹, step like $\{211\}$ microfacets has been observed. Using the present model we have not obtained the faceted phase with large $\{211\}$ pyramids and small $\{011\}$ pyramids as

observed in Pd/W(111)² for prolonged annealing time. This might be due to lack of density fluctuation. So we are going to extend the model including dependence on coverage. The most general extension should base on replacing of the interactions $\epsilon_i^{\alpha\beta}$ by many-body potentials. To construct such potentials, e.g., for Mo-Pd, W-Pd systems, the results of the first-principle calculations could be used¹⁸.

Acknowledgements

I would like to thank prof. Jan Kołaczekiewicz and dr Andrzej Szczepkiewicz for discussions. This work was supported by the Polish State Committee of Scientific Research (KBN) Grant No 2 P0 3B 107 19.

* Electronic address: oleksy@ift.uni.wroc.pl

- ¹ T. E. Madey, C.-H. Nien, K. Pelhos, J. J. Kolodziej, I. M. Abdelrehim, and H.-S. Tao, Surf. Sci. **438**, 191 (1999).
- ² C.-H. Nien, T. E. Madey, Y. W. Tai, T. C. Leung, J. G. Che, and C. T. Chan, Phys. Rev. B **59**, 10335 (1999).
- ³ T. E. Madey, J. Guan, C.-H. Nien, C.-Z. Dong, H.-S. Tao, and R. A. Campbell, Surf. Rev. Lett. **3**, 1315 (1996).
- ⁴ C.-Z. Dong, J. Guan, R. A. Campbell, and T. E. Madey, in *The Structure of Surface IV*, edited by X. Xie, S. Y. Tong, and M. A. van Hove (World Scientific, Singapore, 1994) p. 328.
- ⁵ C.-H. Nien and T. E. Madey, Surf. Sci. **380**, L527 (1997).
- ⁶ C.-Z. Dong, L. Zhang, U. Diebold, and T. E. Madey, Surf. Sci. **322**, 221 (1995).
- ⁷ Ker-Jar Song, J. C. Lin, M. Y. Lai, and Y. L. Wang Surf. Sci. **327**, 17 (1995).
- ⁸ R. Szukiewicz and J. Kołaczekiewicz, *Thermal stability of the Ta (111) surface covered with Pd* (unpublished, submitted to Surface Science).
- ⁹ J. G. Che, C. T. Chan, C. H. Kuo, and T. C. Leung, Phys. Rev. Lett. **79**, 4230 (1997).

- ¹⁰ C. T. Chan, J. G. Che, and T. C. Leung, Progress in Surface Science **59**, 1 (1998).
- ¹¹ H. van Beijeren, Phys. Rev. Lett. **38**, 993 (1977).
- ¹² S. Prestipino, G. Santoro, and E. Tosatti, Phys. Rev. Lett. **75**, 4468 (1995).
- ¹³ G. Mazzeo, E. Carlon, and H. van Beijeren, Phys. Rev. Lett. **74**, 1391 (1995).
- ¹⁴ V. P. Zhdanov and B. Kaseno, Phys. Rev. B **56**, R10067 (1997).
- ¹⁵ G. Santoro, M. Vendruscolo, S. Prestipino, and E. Tosatti, Phys. Rev. B **53**, 13169 (1996).
- ¹⁶ P. C. Searson, R. Li, and K. Sieradzki, Phys. Rev. Lett. **74**, 1395 (1995).
- ¹⁷ M. W. Finnis and J. E. Sinclair, Philos. Mag. A **50**, 45 (1984).
- ¹⁸ Q. Zhang, W. S. Lai, and B. X. Liu, Phys. Rev. B **58**, 14020 (1998).
- ¹⁹ A. Szczepkiewicz and A. Ciszewski, Surf. Sci. **515**, 441 (2002).